

The boiling points of **5** and **6** were determined on a Buchi capillary melting point apparatus and corrected to normal pressure. The boiling point of **7** was measured at several reduced pressures and corrected to 760 nm. The dipole moment of **7** was derived by the method of Guttenheim to be 4.77 D.<sup>28</sup>

**Acknowledgment.** We are grateful to the National Science

Foundation for support of this work.

**Registry No.** **5**, 874-14-6; **6**, 3551-55-1; **7**, 7152-66-1; **8**, 27460-04-4; **9**, 83542-65-8; **11**, 66-22-8; **13**, 51953-19-6; **16**, 51953-14-1.

(28) Shoemaker, D. P.; Garland, C. W. "Experiments in Physical Chemistry"; McGraw-Hill: New York, 1962; pp 51-58.

## Structural Characterization of Channel Inclusion Compounds Formed by Furaltadone Hydrochloride: Comparison to the Crystal and Molecular Structures of Furaltadone Base and Moxnidazole Hydrochloride<sup>1</sup>

Israel Goldberg

Contribution from the Tel-Aviv University, Institute of Chemistry, 69978 Ramat Aviv, Israel.

Received February 22, 1982

**Abstract:** This paper reports new inclusion complexes of furaltadone [5-(morpholinomethyl)-3-[(5-nitrofurfurylidene)-amino]-2-oxazolidinone] hydrochloride with acetic acid, propionic acid, and water as substrate molecules. The inclusion compounds crystallize in the monoclinic space group  $P2_1/c$  ( $Z = 4$ ) and represent channel-type clathrates in which the guest molecules are accommodated in continuous canals running through the crystal parallel to the  $c$  axis. The canals have an approximately cylindrical shape and are lined with oxygen and chlorine nucleophiles; nevertheless, the enclathrated species are translationally disordered in their location in the channel. The crystal structures of the inclusion compounds are compared with those observed for the furaltadone base and moxnidazole hydrochloride. The latter is a closely related species to furaltadone hydrochloride, with an *N*-methylnitroimidazole ring instead of the nitrofur moiety. However, the observed configuration of moxnidazole and, consequently, the relative orientation of its polar groups are different in order to avoid intramolecular steric hindrance. As an apparent result, no clathrate-type channels are formed when a hydrate of moxnidazole hydrochloride crystallizes from water. The solvent-free structure of furaltadone is dominated by characteristic dipole-dipole interactions between molecules located across crystallographic centers of symmetry. Remarkably similar interactions of dipolar "dimerization" are present in the compounds containing furaltadone (but not moxnidazole) hydrochloride; we thus suggest that they are significant to the formation of the observed channel inclusion structures. Relative stability of the inclusion compounds is discussed, and molecular geometries of all the involved species are described in detail. Molecules of acetic acid appear in the channel complexes as isolated monomeric species.

One of the most interesting aspects of host-guest chemistry relates to the formation of crystalline clathrate inclusion compounds in which guest species are enclosed by channels or cages that occur in a given host lattice.<sup>2</sup> Selected series of such inclusion systems have been particularly useful in recent studies of photochemical reactions in the solid state<sup>3</sup> and of selective molecular complexation<sup>4</sup> that is central to biological phenomena. In the course of our investigations into the structural properties of inclusion compounds, we observed that furaltadone hydrochloride,

$C_{13}H_{16}N_4O_6 \cdot HCl$ , an antibacterial agent derived from nitrofur, tends to form clathrate-type complexes when crystallized from various solvents. On the other hand, the closely related species of furaltadone and of moxnidazole hydrochloride (in which the nitrofur moiety is replaced by an *N*-methylnitroimidazole ring) exhibit different habits of crystallization. Since no relevant structural data have previously been reported, and in order to understand the stereochemical features of these phenomena, we decided to investigate a series of crystals in greater detail.

The present account is thus concerned with the crystal structures of three channel inclusion complexes of furaltadone hydrochloride with acetic acid (I), propionic acid (II), and 2 mol of water (III), as well as with those of furaltadone (IV), furaltadone monohydrate (V), and moxnidazole hydrochloride monohydrate (VI). We examine the molecular structures of moxnidazole and furaltadone (in the various environments) moieties and compare their configurational details. There is an emphasis on the characteristic intermolecular interactions found between the furaltadone species that seem to play an important role in the formation of the inclusion structures.

### Experimental Section

The hydrochloric salts of furaltadone and moxnidazole were prepared by TEVA Pharmaceutical Industries, Ltd. Single crystals of the inclusion

(1) A short account of this work has been presented at the Sixth European Crystallographic Meeting, Barcelona, Spain, July 28, 1980. The nontrivial names of furaltadone and moxnidazole are 5-(morpholinomethyl)-3-[(5-nitrofurfurylidene)amino]-2-oxazolidinone and 5-(morpholinomethyl)-3-[1-*N*-methyl-5-nitroimidazolyl-2-methylene]amino]-2-oxazolidinone, respectively.

(2) For a recent review, see, e.g.: MacNicol, D. D.; McKendrick, J. J.; Wilson, D. R. *Chem. Soc. Rev.* 1978, 7, 65-87.

(3) (a) In tri-*o*-thymotide clathrates: Arad-Yellin, R.; Brunle, S.; Green, B. S.; Knosow, M.; Tsoucaris, G. *J. Am. Chem. Soc.* 1979, 101, 7529-7537.

(b) In inclusion complexes of the choleic acids: Popovitz-Biro, R.; Chang, H. C.; Tang, C. P.; Shochet, N. R.; Lahav, M.; Leiserowitz, L. Work presented at the 47th Meeting of the Israel Chemical Society, Rehovot, 28-29 Sept 1980. See also *J. Am. Chem. Soc.* 1978, 100, 2542-2544.

(4) (a) Iwamoto, T. *Isr. J. Chem.* 1979, 18, 240-245. (b) Barrer, R. M.; Shanson, V. H. *J. Chem. Soc., Faraday Trans. 1* 1976, 2348-2354. (c) Cooper, A.; MacNicol, D. D. *J. Chem. Soc., Perkin Trans. 2* 1978, 760-763.

Table I. Summary of Crystal Data and Experimental Parameters

	I	II	III	IV	V	VI
$M_r$	420.8	434.8	396.8	324.3	342.3	392.8
space group	$P2_1/c$	$P2_1/c$	$P2_1/c$	$P2_1/n$	$P1$	$P2_1/c$
$Z$	4	4	4	4	2	4
$a$ , Å	10.212 (1)	10.352 (2)	10.016 (2)	6.465 (2)	6.958 (1)	9.779 (2)
$b$ , Å	17.440 (4)	17.617 (3)	16.742 (5)	24.986 (5)	8.100 (2)	26.142 (4)
$c$ , Å	11.181 (3)	11.290 (9)	11.241 (9)	9.606 (9)	14.823 (3)	6.977 (2)
$\alpha$ , deg	90.0	90.0	90.0	90.0	96.60 (2)	90.0
$\beta$ , deg	93.06 (1)	94.76 (3)	91.68 (3)	99.17 (6)	85.24 (2)	97.74 (2)
$\gamma$ , deg	90.0	90.0	90.0	90.0	104.69 (2)	90.0
$V$ , Å <sup>3</sup>	1988.6	2051.8	1884.2	1531.8	801.5	1767.4
$d_c$ , g cm <sup>-3</sup>	1.405	1.408	1.399	1.406	1.418	1.476
$\lambda$ , Å	0.7107	0.7107	0.7107	0.7107	1.5418	1.5418
crystal size, mm	0.3 × 0.3 × 0.1	<i>a</i>	0.5 × 0.4 × 0.2	0.5 × 0.4 × 0.1	0.4 × 0.2 × 0.2	0.4 × 0.3 × 0.2
2 $\theta$ limits, deg	54	<i>a</i>	54	46	150	150
no. of unique data	3354	<i>a</i>	3316	1846	2953	3335
data with $I \geq 3\sigma_I$	1702	<i>a</i>	2037	1191	2331	2672
refined parameters	284	<i>a</i>	251	208	271	298
$F(000)$ , e	880	<i>a</i>	832	680	360	824
$R$	0.053	<i>a</i>	0.049	0.122	0.046	0.048
"g.o.f.", e	1.64	<i>a</i>	1.32	2.38	1.67	1.80

<sup>a</sup> Not analyzed.

compounds I, II, and III suitable for crystallographic study were obtained upon recrystallization of furaltadone hydrochloride from glacial acetic acid, propionic acid, and water (in the presence of a few drops of 1 N H<sub>2</sub>SO<sub>4</sub>), respectively. Solvent-free crystals of the furaltadone base IV were grown from dimethyl sulfoxide while those of its monohydrate V were obtained from an aqueous solution containing NH<sub>4</sub>OH. Moxnidazole hydrochloride crystallized from water in a monohydrated form VI. The chemical formulas are given in Table I; those of compounds III and IV were confirmed also by chemical analyses.

Diffraction data were measured at room temperature on an Enraf-Nonius CAD-4 diffractometer equipped with a graphite monochromator, employing either Mo or Cu K $\alpha$  radiation and an  $\omega$ -2 $\theta$  scan technique. The cell constants and pertinent details of the experimental conditions are summarized in Table I. For prevention of decomposition, crystals of I and II had to be enclosed within a glass capillary during the collection of data, the latter being very small and poorly diffracting. Since the propionic acid complex, II, appeared to be isomorphous to I and III, detailed study of its structure was postponed to a later date. Possible deterioration of the analyzed crystals was tested by detecting frequently the intensities of standard reflections and was found negligible during the measurements. The data sets were not corrected for absorption and extinction effects. Final refinements were based only on those observations that satisfied the condition  $F_o^2 \geq 3\sigma(F_o^2)$ .

**Structure Determination.** Structures III–VI were solved by a combination of direct methods (MULTAN74 and MULTAN78) and Fourier techniques. The structure determination of the acetic acid complex was based on the assumption that structures I and III are isomorphous, the final atomic coordinates of furaltadone hydrochloride in III being thus used as a starting model of the host lattice in I. Hydrogen atoms attached to the furaltadone or moxnidazole frameworks were introduced in calculated positions and assigned isotropic temperature factors, but their parameters were not refined. The atomic scattering factors for non-hydrogen atoms were taken from ref 5a, those for H from ref 5b.

**Refinement of I and III.** Probable positions of the two water molecules in III were found by difference Fourier calculations based on an isotropically refined heavy-atom model of furaltadone hydrochloride. Subsequent anisotropic refinement of all the non-hydrogen atoms followed by another difference synthesis indicated, however, a significant disorder of the water molecules along a direction parallel to  $c$ . Consequently, each H<sub>2</sub>O was assumed to be disordered between three sites approximately at  $x, y, z$  (major site),  $x, y, z + \delta$ , and  $x, y, z - \delta'$  (minor sites), where  $\delta$  and  $\delta'$  correspond to  $1.0 \pm 0.2$  Å. The following parameters were then included in the refinement: atomic positions of the three oxygen sites, anisotropic  $U_{ij}$  at the major site and isotropic  $U$  at the minor sites, and occupancy factors of each site—their sum being constrained to unity. No reliable positions could be found for the hydrogens of the disordered H<sub>2</sub>O. The final discrepancy factor following convergence is  $R = 0.049$ .

The crystal structure of the acetic acid complex I was derived from that of the isomorphous compound III, the water molecules being ex-

cluded from the initial starting set of coordinates. An isotropic refinement followed by difference Fourier calculations led to the location of one molecule of acetic acid near (in between) the positions previously occupied by water. The results of subsequent anisotropic calculations revealed also features of disorder of the guest molecule along  $c$  similar to those observed in the previous example. A corresponding model of the disorder was then constructed and its parameters were refined, including relative occupancy factors, orientational and positional parameters of the assumedly rigid molecules of acetic acid (this geometric constraint was imposed to minimize correlation effects), and individual anisotropic (at the major site) and isotropic (at the minor sites) temperature factors of the atoms. In the concluding stages of the refinement all atomic parameters were adjusted independently. At convergence  $R$  was 0.056, excluding the disordered hydrogen atoms whose positions were not found. Evidently, the refined occupancy factors associated with the three sites of the postulated disorder of the acetic acid in I are similar to those defined for the water molecules in III, about 0.5, 0.25, and 0.25 at  $x, y, z, x, y, z + \delta$  and  $x, y, z - \delta'$ , respectively (in I,  $\delta, \delta' = 0.06$ ). Only minor deviations from these values occurred when the occupancy factors were refined in an unconstrained manner, indicating that the solvent contents in I and III were determined correctly. However, because of the disorder the spatial distribution of solvent molecules in the actual structures may not obey exactly the space symmetry characteristic to the host lattice.

**Refinement of IV.** All the available crystals of anhydrous furaltadone were of poor quality, and the collected data set contained a large number of intensities below the threshold of  $3\sigma$ . Consequently, the refinement of the structure did not converge well, and it became apparent during the calculations that there exists a significant conformational disorder within the morpholine ring. On the other hand, the remaining part of the molecule appeared to be perfectly ordered and well-defined. Since the geometric features of this structure are particularly significant with respect to the discussion that follows and its solution appeared to be essentially correct, we proceeded with an unconstrained least-squares refinement in spite of the fact that the description of the entire molecule remained clearly still incomplete. (Our attempts at defining a suitable model of the disorder were unsuccessful.) It should thus be kept in mind that the final coordinates of some atoms, particularly those of C(17) through C(23), represent only an average position over a range of energetically preferred conformations. This refinement converged at  $R = 0.12$  for 1252 observations.

**Refinement of V and VI.** The weighted least-squares refinement of both structures converged smoothly at  $R = 0.046$  for V and  $R = 0.048$  for VI. The water molecules (including their H atoms) were clearly located on the corresponding difference maps and then introduced into the refined models.

The final difference Fourier maps showed no indications of incorrectly placed or missing atoms; several relatively high and diffused peaks (ranging from  $-0.6$  to  $+0.8$  e Å<sup>-3</sup>) appeared only in the vicinity of the disordered morpholine ring in IV. Final atomic coordinates for compounds I, III, IV, V, and VI are listed in Tables II–VI, respectively.

## Results and Discussion

**Intramolecular Features.** Figure 1 illustrates the molecular structures of the furaltadone and moxnidazole moieties (taken

(5) (a) "International Tables for X-ray Crystallography"; Kynoch Press: Birmingham, England, 1974; Vol. IV. (b) Stewart, R. F.; Davidson, E. R.; Simpson, W. T. *J. Chem. Phys.* **1965**, *42*, 3175–3187.

Table II. Positional and Isotropic Thermal Parameters of Compound I<sup>a</sup>

atom	x	y	z	$U_{eq}/U, \text{Å}^2$
Cl	0.1720 (1)	0.9583 (1)	0.4142 (1)	0.054
C(1)	0.1821 (5)	0.4475 (3)	0.6394 (4)	0.039
C(2)	0.3031 (5)	0.4682 (3)	0.6112 (5)	0.048
C(3)	0.2921 (5)	0.5461 (4)	0.5795 (5)	0.053
C(4)	0.1641 (5)	0.5667 (3)	0.5891 (4)	0.038
O(5)	0.0943 (3)	0.5054 (2)	0.6255 (3)	0.035
N(6)	0.1333 (4)	0.3762 (2)	0.6841 (4)	0.041
O(7)	0.0205 (4)	0.3732 (2)	0.7076 (4)	0.063
O(8)	0.2122 (5)	0.3251 (2)	0.6942 (4)	0.074
C(9)	0.1007 (5)	0.6394 (3)	0.5684 (5)	0.041
N(10)	-0.0208 (4)	0.6470 (2)	0.5867 (4)	0.037
N(11)	-0.0742 (4)	0.7177 (2)	0.5634 (4)	0.040
C(12)	-0.0098 (6)	0.7814 (3)	0.5083 (5)	0.044
C(13)	-0.1217 (5)	0.8399 (3)	0.4959 (5)	0.041
O(14)	-0.2388 (4)	0.7974 (2)	0.5259 (3)	0.050
C(15)	-0.2069 (5)	0.7274 (3)	0.5676 (4)	0.040
O(16)	-0.2852 (4)	0.6824 (2)	0.6019 (3)	0.053
C(17)	-0.1368 (5)	0.8709 (3)	0.3719 (5)	0.036
N(18)	-0.2197 (4)	0.9421 (2)	0.3635 (3)	0.031
C(19)	-0.3650 (5)	0.9255 (3)	0.3583 (5)	0.041
C(20)	-0.4394 (5)	1.0001 (3)	0.3420 (5)	0.047
O(21)	-0.4052 (3)	1.0392 (2)	0.2378 (3)	0.051
C(22)	-0.2695 (5)	1.0585 (3)	0.2482 (5)	0.042
C(23)	-0.1853 (5)	0.9884 (3)	0.2568 (5)	0.038
O(24)	0.6331 (8)	0.3411 (4)	0.1653 (7)	0.057
O(25)	0.7163 (11)	0.2405 (6)	0.1015 (9)	0.099
C(26)	0.5164 (12)	0.2279 (7)	0.1891 (12)	0.068
C(27)	0.6330 (10)	0.2706 (6)	0.1492 (10)	0.045
O(24*)	0.6494 (20)	0.3420 (13)	0.2100 (19)	0.095
O(25*)	0.7570 (23)	0.2499 (13)	0.1866 (20)	0.105
C(26*)	0.5405 (24)	0.2285 (15)	0.2600 (23)	0.067
C(27*)	0.6519 (37)	0.2740 (22)	0.2097 (32)	0.107
O(24+)	0.6248 (19)	0.3430 (12)	0.1079 (17)	0.080
O(25+)	0.6866 (25)	0.2578 (15)	0.0224 (23)	0.120
C(26+)	0.5086 (26)	0.2237 (15)	0.1273 (23)	0.060
C(27+)	0.6194 (33)	0.2722 (21)	0.0933 (30)	0.091
H(2)	0.3867	0.4345	0.6107	0.050
H(3)	0.3691	0.5818	0.5560	0.050
H(9)	0.1529	0.6867	0.5398	0.050
H(12A)	0.0317	0.7676	0.4306	0.050
H(12B)	0.0702	0.8027	0.5660	0.050
H(13)	-0.1069	0.8882	0.5486	0.050
H(17A)	-0.1780	0.8298	0.3167	0.050
H(17B)	-0.0449	0.8834	0.3420	0.050
H(18)	-0.2011	0.9731	0.4422	0.050
H(19A)	-0.3926	0.8965	0.4315	0.050
H(19B)	-0.3887	0.8909	0.2834	0.050
H(20A)	-0.4162	1.0340	0.4170	0.050
H(20B)	-0.5382	0.9906	0.3396	0.050
H(22A)	-0.2489	1.0901	0.3278	0.050
H(22B)	-0.2429	1.0928	0.1797	0.050
H(23A)	-0.0877	1.0018	0.2594	0.050
H(23B)	-0.2049	0.9563	0.1789	0.050

<sup>a</sup> The occupancy factors of atoms O(24)-C(27), O(24\*)-C(27\*), and O(24+)-C(27+) are 0.51 (1), 0.25 (1), and 0.24 (1), respectively.

from I and VI) along with the atom-labeling scheme. The covalent bond lengths and angles obtained for the furaltadone framework are compared in Tables VII and VIII, excluding those of the partially disordered compound IV, which are less reliable. Most of the individual parameters have very similar values in the three other structures I, III, and V, exhibiting no extraordinary features. The only significant exception from this trend involves atom N(18), which becomes protonated upon formation of the hydrochloric salt. Thus, the C-N(18) bonds are consistently shorter and the sum of the three bond angles around the nitrogen is smaller in the neutral base (average 1.464 Å and 328.4°, respectively) than in the charged molecules (average 1.500 Å and 333.5°, respectively). Molecular dimensions of the moxnidazole framework in structure VI are shown in Table IX. They indicate that within the *N*-methylimidazole ring  $\pi$  electrons are partially delocalized. The distribution of bond distances and angles in the remaining

Table III. Positional and Isotropic Thermal Parameters of Compound III<sup>a</sup>

atom	x	y	z	$U_{eq}/U, \text{Å}^2$
Cl	0.1884 (1)	0.9527 (1)	0.4109 (1)	0.053
C(1)	0.1892 (5)	0.4402 (3)	0.6389 (4)	0.042
C(2)	0.3120 (5)	0.4615 (4)	0.6070 (5)	0.051
C(3)	0.3010 (5)	0.5418 (4)	0.5726 (5)	0.053
C(4)	0.1718 (5)	0.5632 (3)	0.5865 (4)	0.042
O(5)	0.0992 (3)	0.5002 (2)	0.6261 (3)	0.040
N(6)	0.1423 (5)	0.3677 (3)	0.6850 (4)	0.051
O(7)	0.0250 (4)	0.3622 (2)	0.7127 (3)	0.061
O(8)	0.2240 (4)	0.3128 (2)	0.6944 (4)	0.070
C(9)	0.1052 (5)	0.6384 (3)	0.5636 (4)	0.042
N(10)	-0.0192 (4)	0.6463 (2)	0.5836 (3)	0.038
N(11)	-0.0736 (4)	0.7194 (2)	0.5576 (3)	0.040
C(12)	-0.0071 (5)	0.7863 (3)	0.5051 (5)	0.046
C(13)	-0.1210 (5)	0.8469 (3)	0.4952 (4)	0.043
O(14)	-0.2397 (4)	0.8038 (2)	0.5301 (3)	0.051
C(15)	-0.2071 (5)	0.7298 (3)	0.5683 (4)	0.042
O(16)	-0.2883 (3)	0.6830 (2)	0.6020 (3)	0.051
C(17)	-0.1373 (5)	0.8783 (3)	0.3704 (4)	0.039
N(18)	-0.2273 (4)	0.9497 (2)	0.3615 (3)	0.034
C(19)	-0.3727 (5)	0.9293 (3)	0.3547 (5)	0.048
C(20)	-0.4538 (5)	1.0052 (4)	0.3407 (5)	0.060
O(21)	-0.4170 (4)	1.0484 (3)	0.2380 (3)	0.063
C(22)	-0.2809 (5)	1.0718 (3)	0.2491 (5)	0.051
C(23)	-0.1921 (5)	0.9997 (3)	0.2568 (4)	0.043
O(W1)	0.432 (1)	0.7357 (8)	0.621 (1)	0.105
O(W2)	0.320 (1)	0.7206 (7)	0.881 (1)	0.118
O(W1*)	0.432 (2)	0.717 (1)	0.527 (2)	0.111
O(W1+)	0.454 (2)	0.758 (1)	0.724 (2)	0.106
O(W2*)	0.318 (2)	0.714 (1)	0.815 (2)	0.106
O(W2+)	0.324 (2)	0.710 (1)	0.956 (2)	0.095
H(2)	0.395	0.426	0.608	0.050
H(3)	0.376	0.577	0.542	0.050
H(9)	0.160	0.686	0.532	0.050
H(12A)	0.030	0.772	0.423	0.050
H(12B)	0.072	0.807	0.556	0.050
H(13)	-0.106	0.895	0.551	0.050
H(17A)	-0.176	0.834	0.317	0.050
H(17B)	-0.047	0.893	0.339	0.050
H(18)	-0.215	0.988	0.435	0.050
H(19A)	-0.399	0.899	0.429	0.050
H(19B)	-0.391	0.892	0.283	0.050
H(20A)	-0.440	1.041	0.413	0.050
H(20B)	-0.554	0.992	0.334	0.050
H(22A)	-0.266	1.108	0.324	0.050
H(22B)	-0.257	1.106	0.177	0.050
H(23A)	-0.096	1.016	0.263	0.050
H(23B)	-0.203	0.966	0.182	0.050

<sup>a</sup> The refined occupancy factors of atoms O(W1), O(W2), O(W1\*), O(W1+), O(W2\*), and O(W2+) are 0.45 (1), 0.47 (1), 0.275, 0.275, 0.265, and 0.265, respectively.

parts of the molecule is very similar to that observed for the furaltadone analogues. A bibliographic search through the Cambridge Data Files<sup>6</sup> reveals that detailed structural data have not yet been published for any derivative of these species.

The overall conformations of the furaltadone molecules in I, III, and V are very much alike, the [(5-nitrofururylidene)-amino]-2-oxazolidinone moiety being approximately planar and the morpholine ring adopting a chair conformation. In compound IV the major molecular fragment exhibits similar features of planarity, but the refined atomic positions of the disordered morpholine resemble an arrangement of a twisted boat. Least-squares calculations of the equations of the plane defined by the fragment C(1)-O(16) in the four compounds show that the displacements of individual atoms from this plane are within  $\pm 0.1$  Å in III and IV and within  $\pm 0.2$  Å in I and V. The moxnidazole compound consists also of a nearly planar fragment extending from N(1) through O(17) and a morpholinomethyl group of a chairlike geometry.

(6) Kennard, O.; Watson, D.; Allen, F.; Motherwell, W.; Town, W.; Rodgers, J. *Chem. Br.* 1975, 11, 213-216.

Table IV. Positional and Isotropic Thermal Parameters of Compound IV

atom	x	y	z	$U_{eq}/\text{\AA}^2$
C(1)	0.3379 (18)	0.4138 (4)	0.9986 (13)	0.061
C(2)	0.1274 (18)	0.4177 (5)	0.9877 (13)	0.070
C(3)	0.0663 (16)	0.4532 (5)	0.8791 (13)	0.067
C(4)	0.2433 (16)	0.4700 (4)	0.8323 (12)	0.056
O(5)	0.4131 (10)	0.4451 (3)	0.9056 (8)	0.054
N(6)	0.4906 (16)	0.3821 (4)	1.0900 (11)	0.082
O(7)	0.6626 (15)	0.3881 (4)	1.0803 (11)	0.108
O(8)	0.4205 (16)	0.3570 (4)	1.1737 (11)	0.115
C(9)	0.2731 (16)	0.5070 (5)	0.7216 (12)	0.057
N(10)	0.4554 (12)	0.5172 (3)	0.6955 (10)	0.054
N(11)	0.4698 (13)	0.5542 (4)	0.5949 (11)	0.066
C(12)	0.3047 (16)	0.5871 (5)	0.5226 (14)	0.070
C(13)	0.4262 (25)	0.6214 (7)	0.4339 (18)	0.119
O(14)	0.6395 (10)	0.6076 (3)	0.4715 (9)	0.074
C(15)	0.6606 (15)	0.5674 (5)	0.5663 (12)	0.059
O(16)	0.8224 (11)	0.5475 (4)	0.6097 (10)	0.084
C(17)	0.3662 (21)	0.6670 (5)	0.3803 (17)	0.097
N(18)	0.4573 (14)	0.7028 (4)	0.2995 (13)	0.083
C(19)	0.6371 (28)	0.6985 (7)	0.2614 (20)	0.134
C(20)	0.7272 (26)	0.7387 (7)	0.1807 (19)	0.130
O(21)	0.6125 (18)	0.7812 (4)	0.1290 (12)	0.128
C(22)	0.4592 (28)	0.7887 (7)	0.1891 (20)	0.136
C(23)	0.3563 (26)	0.7464 (7)	0.2505 (21)	0.137
H(2)	0.036	0.399	1.047	0.060
H(3)	-0.078	0.465	0.840	0.060
H(9)	0.148	0.525	0.666	0.060
H(12A)	0.238	0.609	0.590	0.060
H(12B)	0.193	0.565	0.463	0.060
H(13)	0.373	0.614	0.331	0.060
H(17A)	0.345	0.689	0.467	0.060
H(17B)	0.224	0.660	0.322	0.060
H(19A)	0.630	0.664	0.204	0.060
H(19B)	0.741	0.694	0.354	0.060
H(20A)	0.770	0.719	0.096	0.060
H(20B)	0.854	0.753	0.245	0.060
H(22A)	0.347	0.806	0.115	0.060
H(22B)	0.509	0.815	0.271	0.060
H(23A)	0.239	0.734	0.174	0.060
H(23B)	0.298	0.763	0.335	0.060

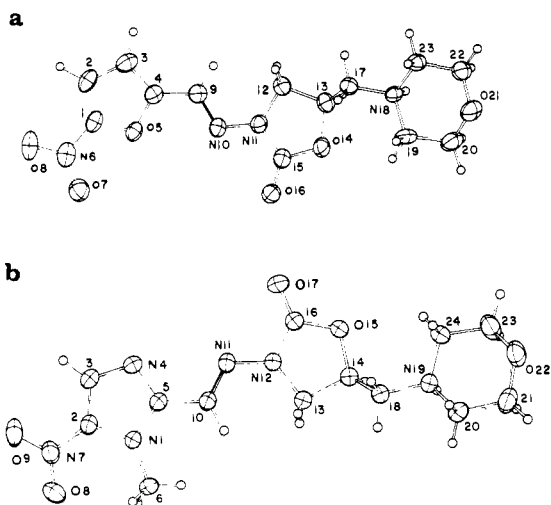


Figure 1. Molecular formulas of the (a) furaltadone and (b) moxnidazole moieties showing the atom numbering scheme (taken from structures I and VI).

Another aspect of the molecular configuration deserves attention. In the four observed structures containing the furaltadone moiety the polar  $\text{NO}_2$  substituent is oriented in a direction parallel to the carbonyl bond  $\text{C}(15)=\text{O}(16)$ . A similar relative orientation of the heterocyclic rings in moxnidazole species would probably cause a severe steric crowding between the *N*-methyl substituent and the central part of the molecule (for example, the nonbonding  $\text{C}(6)\cdots\text{N}(11)$  distance would become about 2.74 Å); this is relieved

Table V. Positional and Isotropic Thermal Parameters of Compound V

atom	x	y	z	$U_{eq}/\text{\AA}^2$
C(1)	0.5864 (5)	0.5548 (4)	0.7453 (2)	0.050
C(2)	0.7527 (5)	0.5498 (5)	0.7848 (2)	0.056
C(3)	0.8444 (5)	0.4444 (5)	0.7222 (2)	0.055
C(4)	0.7278 (4)	0.3944 (4)	0.6500 (2)	0.046
O(5)	0.5643 (3)	0.4615 (3)	0.6632 (1)	0.046
N(6)	0.4344 (4)	0.6392 (4)	0.7753 (2)	0.061
O(7)	0.2945 (4)	0.6205 (3)	0.7261 (2)	0.075
O(8)	0.4524 (5)	0.7258 (4)	0.8488 (2)	0.091
C(9)	0.7528 (5)	0.2891 (4)	0.5669 (2)	0.047
N(10)	0.6132 (4)	0.2393 (3)	0.5117 (2)	0.045
N(11)	0.6503 (4)	0.1375 (4)	0.4361 (2)	0.049
C(12)	0.8344 (5)	0.0891 (5)	0.4082 (2)	0.054
C(13)	0.7724 (5)	-0.0370 (5)	0.3242 (2)	0.056
O(14)	0.5790 (3)	-0.0121 (3)	0.3041 (1)	0.055
C(15)	0.5097 (5)	0.0830 (4)	0.3733 (2)	0.048
O(16)	0.3473 (3)	0.1118 (3)	0.3763 (2)	0.060
C(17)	0.9204 (5)	-0.0040 (5)	0.2456 (2)	0.056
N(18)	0.9000 (4)	-0.1502 (4)	0.1757 (2)	0.056
C(19)	1.0815 (6)	-0.1229 (5)	0.1161 (2)	0.064
C(20)	1.0649 (7)	-0.2678 (6)	0.0418 (3)	0.081
O(21)	0.8982 (5)	-0.2843 (4)	-0.0105 (2)	0.078
C(22)	0.7208 (7)	-0.3096 (6)	0.0461 (3)	0.084
C(23)	0.7299 (6)	-0.1659 (5)	0.1210 (2)	0.071
O(W)	0.2125 (4)	0.3445 (4)	0.5280 (2)	0.075
H(2)	0.802	0.609	0.844	0.055
H(3)	0.971	0.409	0.729	0.055
H(9)	0.879	0.258	0.558	0.055
H(12A)	0.876	0.031	0.459	0.055
H(12B)	0.940	0.192	0.395	0.055
H(13)	0.763	-0.167	0.336	0.060
H(17A)	1.062	0.024	0.270	0.060
H(17B)	0.902	0.107	0.219	0.060
H(19A)	1.200	-0.112	0.153	0.075
H(19B)	1.106	-0.006	0.089	0.075
H(20A)	1.051	-0.384	0.070	0.075
H(20B)	1.188	-0.249	0.000	0.075
H(22A)	0.702	-0.424	0.074	0.075
H(22B)	0.598	-0.320	0.010	0.075
H(23A)	0.608	-0.192	0.161	0.075
H(23B)	0.742	-0.053	0.092	0.075
H(W1)	0.287	0.042	0.569	0.070
H(W2)	0.309	0.292	0.500	0.070

by a  $180^\circ$  rotation of the *N*-methylnitroimidazole fragment about the  $\text{C}(5)-\text{C}(10)$  bond. Furthermore, iterative EH calculations<sup>7</sup> carried out on neutral molecular models of furaltadone and moxnidazole provided the following indications: (a) the observed ground-state configuration of moxnidazole is more stable by about 8.3 kcal/mol than a configuration resembling the structure of furaltadone; and (b) the dipolarity of both the furaltadone and moxnidazole species is largest in their respective observed configurations—upon rotation of the terminal ring with respect to the remaining part of the molecular skeleton the calculated dipole moment decreases from 13.8 to 6.5 D in furaltadone and from 11.7 to 9.7 D in moxnidazole.<sup>8</sup> The packing modes exhibited by the furaltadone species are related below to its electrostatic properties.

**Crystal Structures.** The crystal structure of the homomolecular compound IV is of particular interest because it provides an illustration of the characteristic interactions that exist between the furaltadone units in the solid. This structure can be described as composed of stacks of molecules that extend parallel to the *c* axis (Figure 2a). Within the stacks, adjacent molecules appear to associate by dipolar interactions either mainly between the oxazolidinone rings (mode A) or mainly between the (nitro-

(7) Rein, R.; Clarke, G. A.; Harris, F. E. "Quantum Aspects of Heterocyclic Compounds in Chemistry and Biochemistry"; The Israel Academy of Sciences and Humanities: Jerusalem, 1970; pp 86-115.

(8) In view of the approximations involved in these calculations, the data given in text should be considered only on a qualitative relative scale.

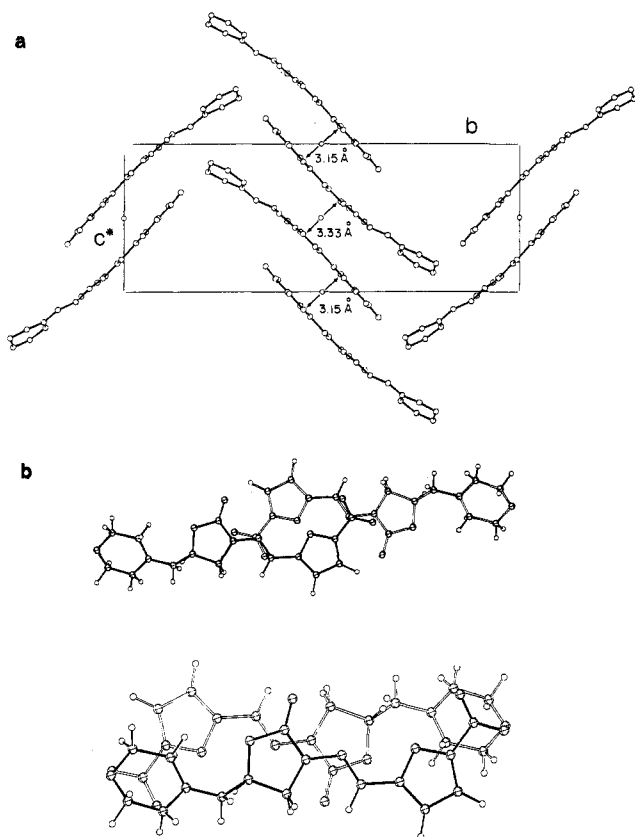


**Figure 2.** (a) Crystal structure of compound IV viewed down the *a* axis, and (b) face-on view of the two modes of intermolecular overlap at 3.15 and 3.33 Å along the stacks.

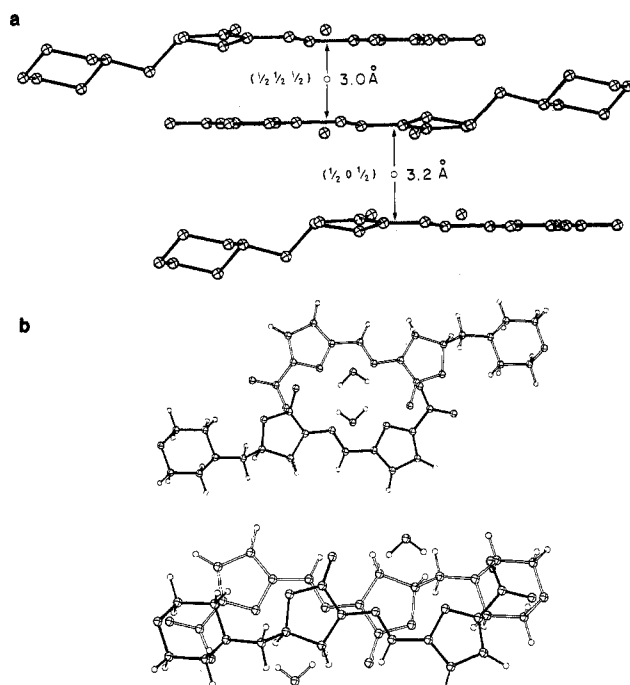


**Figure 3.** Illustration of the (a) stacking and (b) overlap interactions in the crystal structure of furaltadone monohydrate (V).

furfurylidene)amino fragments (mode B) with the morpholine rings located outside the region of the overlap (Figure 2b). We estimated very roughly, using the Coulomb equation<sup>9</sup> for the dipolar bonds and partial atomic charges from the iterative EH

(9) The Coulomb interactions were obtained in kcal/mol by the equation  $E = 332q_1q_2/Dr$ , in which  $q_i$  = fractional charge on an atom,  $D$  = dielectric constant (taken as 1.0), and  $r$  = distance in Å.

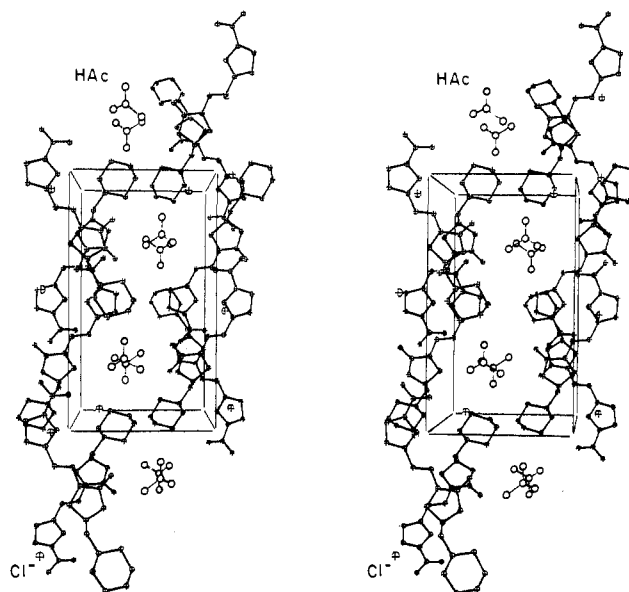


**Figure 4.** Stereoview of the furaltadone hydrochloride structure, approximately down *c*, with the acetic acid molecule included.

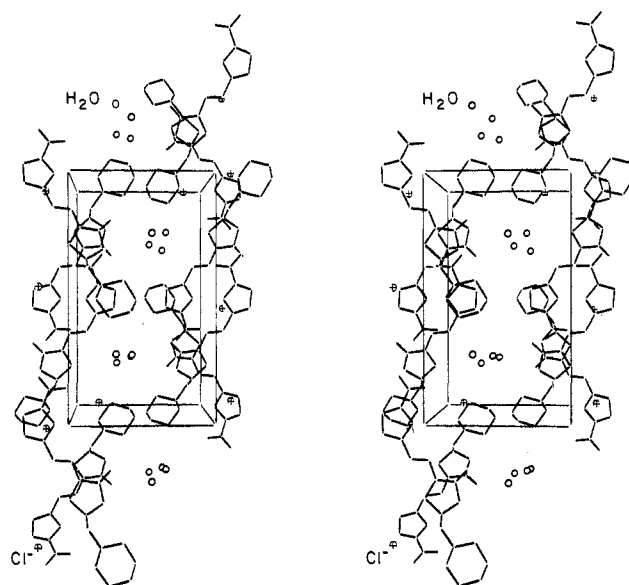


**Figure 5.** Stereoview of the channel inclusion structure formed by furaltadone hydrochloride with 2 mol of water.

calculations,<sup>7</sup> that the contribution of electrostatic stabilization to the interaction energy between molecules pairing in mode B (with an interplanar distance of 3.15 Å) is greater than that between molecules pairing in mode A (with an interplanar distance of 3.33 Å) by about 1.6 kcal/mol.

The crystal structure of furaltadone monohydrate V, illustrated in Figure 3a, is also characterized by a relatively dense packing. Molecules of furaltadone are stacked along the *b* axis in the form of dipolarly coupled dimers across the  $1/2, 1/2, 1/2$  centers of inversion. The mean separation between the planar fragments within such dimers is 3.0 Å, some of the individual nonbonding distances being relatively short (e.g., O(7)⋯C(15) = 2.94 Å). The average interplanar distance between molecules related by inversion at  $1/2, 0, 1/2$  is 3.2 Å. The above data correspond to two different modes of intermolecular overlap (Figure 3b), resembling previous observations in the anhydrous compound; in both structures stronger electrostatic interactions appear to be associated with only partial overlap of the molecular entities.

Within layers roughly perpendicular to the stacking axis, the H<sub>2</sub>O molecules are effectively hydrogen bonded to and enclosed between furaltadone species displaced along *a*. Relevant distances and angles associated with the hydrogen bonds are as follows:

Table VI. Positional and Isotropic Thermal Parameters of Compound VI

atom	x	y	z	$U_{eq}/\text{\AA}^2$
N(1)	0.4861 (3)	0.3377 (1)	0.2296 (4)	0.037
C(2)	0.6053 (3)	0.3142 (1)	0.1886 (5)	0.041
C(3)	0.7016 (4)	0.3513 (1)	0.1823 (6)	0.049
N(4)	0.6479 (3)	0.3971 (1)	0.2172 (5)	0.048
C(5)	0.5168 (3)	0.3879 (1)	0.2428 (5)	0.038
C(6)	0.3558 (4)	0.3128 (1)	0.2595 (6)	0.049
N(7)	0.6207 (3)	0.2615 (1)	0.1580 (5)	0.052
O(8)	0.5301 (3)	0.2313 (1)	0.1910 (5)	0.076
O(9)	0.7277 (3)	0.2479 (1)	0.0972 (5)	0.074
C(10)	0.4191 (3)	0.4282 (1)	0.2749 (5)	0.039
N(11)	0.4600 (3)	0.4740 (1)	0.2684 (4)	0.041
N(12)	0.3693 (3)	0.5116 (1)	0.2967 (4)	0.041
C(13)	0.2253 (3)	0.5055 (1)	0.3150 (6)	0.044
C(14)	0.1820 (3)	0.5608 (1)	0.3373 (5)	0.041
O(15)	0.2934 (2)	0.5913 (1)	0.2758 (4)	0.049
C(16)	0.4050 (3)	0.5613 (1)	0.2643 (5)	0.043
O(17)	0.5148 (3)	0.5775 (1)	0.2331 (5)	0.060
C(18)	0.0469 (3)	0.5722 (1)	0.2156 (5)	0.040
N(19)	-0.0219 (3)	0.6199 (1)	0.2725 (4)	0.037
C(20)	-0.1700 (3)	0.6214 (1)	0.1819 (6)	0.049
C(21)	-0.2378 (4)	0.6695 (2)	0.2400 (6)	0.059
O(22)	-0.1680 (3)	0.7138 (1)	0.1861 (4)	0.062
C(23)	-0.0302 (4)	0.7140 (2)	0.2817 (7)	0.062
C(24)	0.0492 (4)	0.6682 (1)	0.2246 (6)	0.048
Cl	-0.0440 (1)	0.6115 (0)	0.7015 (1)	0.050
O(W)	0.7521 (3)	0.4999 (1)	0.1710 (5)	0.078
H(3)	0.796	0.345	0.165	0.050
H(10)	0.325	0.418	0.295	0.050
H(13A)	0.209	0.483	0.421	0.050
H(13B)	0.178	0.491	0.198	0.050
H(18A)	-0.016	0.544	0.228	0.050
H(18B)	0.057	0.575	0.068	0.050
H(20A)	-0.215	0.591	0.220	0.050
H(20B)	-0.172	0.620	0.031	0.050
H(21A)	-0.238	0.669	0.391	0.050
H(21B)	-0.340	0.670	0.170	0.050
H(23A)	-0.031	0.714	0.426	0.050
H(23B)	0.014	0.748	0.251	0.050
H(24A)	0.144	0.668	0.301	0.050
H(24B)	0.050	0.669	0.083	0.050
H(14)	0.173	0.569	0.479	0.050
H(19)	-0.019	0.620	0.407	0.050
H(6A)	0.326	0.287	0.140	0.050
H(6B)	0.292	0.340	0.268	0.050
H(6C)	0.372	0.289	0.378	0.050
H(W1)	0.850	0.494	0.186	0.050
H(W2)	0.722	0.464	0.168	0.050

O(W)···O(16) (at  $x, y, z$ ) = 3.01 Å (H···O = 2.3 Å) and O(W)···H···O(16) = 138°; O(W)···O(5) (at  $x, y, z$ ) = 3.18 Å (H···O = 2.4 Å) and O(W)···H···O(5) = 145°; O(W)···C(9) (at  $x - 1, y, z$ ) = 3.13 Å (O···H = 2.3 Å) and O(W)···H···C(9) = 148°.

The molecular packing of the acetic acid and water inclusion compounds I and III, shown in Figures 4 and 5, respectively, is essentially the same. The two crystal structures can be described as composed of layers of the furaltadone hydrochloride species that extend parallel to the (100) plane. While it is not possible to achieve a satisfactory close arrangement of the ion pairs in the form of continuous stacks that would resemble the packing modes observed for the neutral base in the previous examples, the pattern of dipolarly coupled dimers of the furaltadone moiety found in structure IV (mode B, see above) persists to a remarkable extent within these layers (Figure 6). In fact the dipolar interactions seem even more pronounced in the inclusion compounds (between molecules related by inversion at 0, 0, 0 or 0,  $1/2, 1/2$ ) than in IV, the mean interplanar distance between the similarly overlapping fragments C(1)–O(16) being reduced from 3.15 Å in IV to 3.03–3.04 Å in I and III. The similarity relationship that exists between the intermolecular arrangements in different crystalline environments emphasizes the significance of the specific electrostatic interactions in structures containing the furaltadone species. (A similar type of relationship has been found in various

crystals involving polar molecules such as that of benzo[*c*]cinnoline.<sup>10</sup>)

The layers referred to above are also characterized by an efficient packing of molecules related to each other by the screw axis and glide plane elements of symmetry. This is reflected in several relatively short intermolecular contacts, for example, (a) between the nucleophilic sites O(5) and O(7) at  $x, y, z$  and the CH<sub>2</sub>(22)–CH<sub>2</sub>(23) fragment at  $x, 3/2 - y, z + 1/2$  and (b) between O(8) at  $x, y, z$  and C(15) at  $-x, y - 1/2, 3/2 - z$ . The corresponding nonbonding distances are as follows: O(5)···C(23), 3.28 Å in I and 3.30 Å in III; O(7)···C(22), 3.25 Å in I and 3.29 Å in III; O(7)···C(23), 3.27 Å in I and 3.22 Å in III; O(8)···C(15), 3.16 Å in I and 3.02 Å in III. The latter represents an intermolecular O···C=O interaction,<sup>11</sup> the O(8)···C(15)=O(16) approach angles being 92° in I and 88° in III.

Adjacent layers are separated by about 10 Å, their packing along the  $a$  axis inducing channels in the corresponding crystals that are occupied by the guest molecules (either acetic acid or water). The two channels in the unit cell extend along  $c$  and center at  $x = 0.37, y = 0.73, x = 0.63$  and  $y = 0.27$ . Atoms O(7) and O(16) and the chloride ions are located on the channel walls and thus impart a hydrophilic character to the structure of the host. In both crystal structures I and III the guest species appear to be disordered within the channels. The structural model most consistent with the diffraction data suggests that each molecule of acetic acid or water is disordered between three different sites displaced along  $c$  by 0.7–1.0 Å from each other. On the other hand, the crystallographic results can assumedly be explained also in terms of a broad translational motion of the guests within the channels or by an intermediate model between these two extremes.<sup>12</sup>

In structure III the two independent water molecules form continuous chains within the channels with alternating O···O distances of 2.98 and 3.17 Å. The interaction of the guest with the channel walls is preferentially between O(W1) and O(16) at 2.95 Å and between O(W2) and Cl<sup>-</sup> at 3.21 Å. However, the directions of the hydrogen bonds involving the water molecules were not defined because of their apparent disorder in this structure. When the 2 mol of water is replaced by 1 mol of acetic acid, the channels formed in structure I become wider to accommodate the larger molecules of the guest. The major expansion of the lattice (4.2%) is along  $b$ , mainly due to a slight longitudinal translation between the dipolarly coupled pairs of the furaltadone moiety but with no significant effect on the overlap interactions within each pair.

Molecules of the acetic acid are stacked along the channels with rather large separations between adjacent entities, their molecular planes forming an angle of 27° with the channel axis. They exhibit translational disorder (broad motions) similar to that (those) found in the water complex. Considering the main sites of the disordered model, the mean planes of neighboring species are separated alternately by 4.74 and 4.94 Å, all interatomic distances involved being larger than 4.9 Å. On the other hand, the shortest intermolecular distances that reflect on the interaction of the guest with the host lattice include the following: O(24)···Cl<sup>-</sup>, 3.02 Å, O(24)···CH<sub>2</sub>(19), 3.11 Å, O(25)···CH(9), 3.25 Å, and CH<sub>3</sub>(26)···O(8), 3.24 Å. The chloride ion is thus involved simultaneously in two very significant interactions: with NH(18)<sup>+</sup> within the ion pair at 3.05 Å and with one of the carboxy oxygens of the acetic acid at 3.02 Å.<sup>13</sup> Finally, in view of the fact that mono-

(10) Shaanan, B.; Shmueli, U.; Colapietro, M. *Acta Crystallogr., Sect. B* 1982, B38, 818–824.

(11) Bürgi, H. B.; Dunitz, J. D.; Shefter, E. *Acta Crystallogr., Sect. B* 1974, B30, 1517–1527.

(12) An extensive discussion of similar phenomena of "molecular motion" in cyclophosphazene clathrates is given by Allcock et al. (Allcock, H. R.; Allen, R. W.; Bissell, E. C.; Smeltz, L. A.; Teeter, M. *J. Am. Chem. Soc.* 1976, 98, 5120–5125).

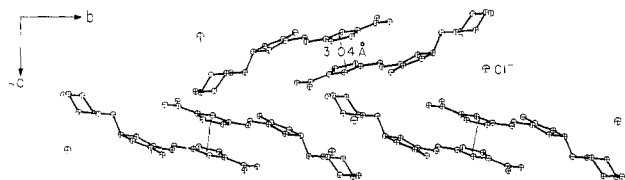


**Figure 6.** Illustration of individual molecular layers in the host lattice of furaltadone hydrochloride; arrows indicate the dipolarly coupled moieties.

carboxylic acids are known to form almost invariably hydrogen-bonded carboxy dimers in the solid,<sup>14</sup> inclusion complex I is a rather unique example of a solid structure that contains discrete molecules of the acetic acid guest. This is due to the effect of enclathration within a host lattice of specified space symmetry as well as the apparent interaction of individual molecules with the  $\text{Cl}^-$  ions.

The intermolecular interactions and molecular disorder described above indicate that the binding between host and guest is rather weak. Consequently, crystals of I tend to deteriorate slowly at ambient room temperature, due to diffusion of the acetic acid into the surrounding atmosphere. In fact, the acid molecules can easily be replaced by water in the clathrate system, as the water complex is considerably more stable under normal conditions. Deterioration of structure III occurs, however, at higher temperatures. We find that the crystals lose rapidly 1 mol of water when their temperature is raised to about 80 °C. The escape of the guest species from compounds I and III has only a minor effect on the overall crystal structure determined by furaltadone hydrochloride; this has been indicated by powder diffraction spectra. Nevertheless, all our efforts to obtain large ( $\geq 0.1$  mm in diameter) single crystals of the free or monohydrated host were unsuccessful.

Moxnidazole hydrochloride crystallizes from aqueous solutions in a monohydrated form, VI. The packing arrangement shown in Figure 7 can be conveniently described in terms of stacked layers that lie parallel to the (001) plane at  $z = 1/4$  and  $z = 3/4$ . Within each layer the  $\text{Cl}^-$  ions and water molecules are contained in local voids between adjacent moieties of moxnidazole. The 1:1 stoichiometry between the hydrochloric salt and the solvent is clearly associated with the formation of relatively strong linear hydrogen bonds from every molecule of water to N(4) of the nearest moxnidazole unit with  $\text{N}(4)\cdots\text{O}(\text{W}) = 2.91$  Å. Evidently, there are no channels in this structure and no disorder of the solvent species (the principal squared amplitudes of thermal vibration of O(W) are 0.060, 0.066, and 0.111 Å). Within the ion pair the  $\text{Cl}^-\cdots\text{NH}(18)^+$  distance is 3.04 Å. All other intermolecular distances are longer than or approximately equal to the sums of the corresponding van der Waals radii.

We tend to believe that the observed differences in crystal packing of the hydrochloric salts of furaltadone and moxnidazole should be attributed mostly to the marked variations in molecular configuration and dipolarity of the two moieties. Effective dipolar coupling is present in crystals containing the free furaltadone base. It persists in the inclusion compounds I and III formed by the furaltadone hydrochloride species but not in structure VI, which contains the moxnidazole analogue. In this respect, the present study provides an interesting example of specific intermolecular interactions other than hydrogen bonding that can play an important role in the formation of clathrate inclusion compounds.<sup>15</sup>

(13) It should be kept in mind that the intermolecular distances given in the text were determined with low accuracy due to the disorder. The geometry of the refined structure of acetic acid at the main site is characterized by the following bond distances and angles:  $\text{C}(27)\text{--}\text{O}(24) = 1.24(1)$  Å,  $\text{C}(27)\text{--}\text{O}(25) = 1.15(2)$  Å,  $\text{C}(27)\text{--}\text{C}(26) = 1.49(2)$  Å,  $\text{O}(24)\text{--}\text{C}(27)\text{--}\text{O}(25) = 122(1)^\circ$ ,  $\text{O}(24)\text{--}\text{C}(27)\text{--}\text{C}(26) = 116(1)^\circ$ , and  $\text{O}(25)\text{--}\text{C}(27)\text{--}\text{C}(26) = 122(1)^\circ$ . No reliable indication is provided by these data with respect to the actual distribution of  $\pi$ -electron density in the carboxy group.

(14) Leiserowitz, L. *Acta Crystallogr., Sect. B* 1976, B32, 775–802.

(15) The role of hydrogen bonding in clathrates has recently been discussed by Hardy et al. (Hardy, A. D. U.; McKendrick, J. J.; MacNicol, D. D.; Wilson, D. R. *J. Chem. Soc., Perkin Trans. 2* 1979, 729–734).

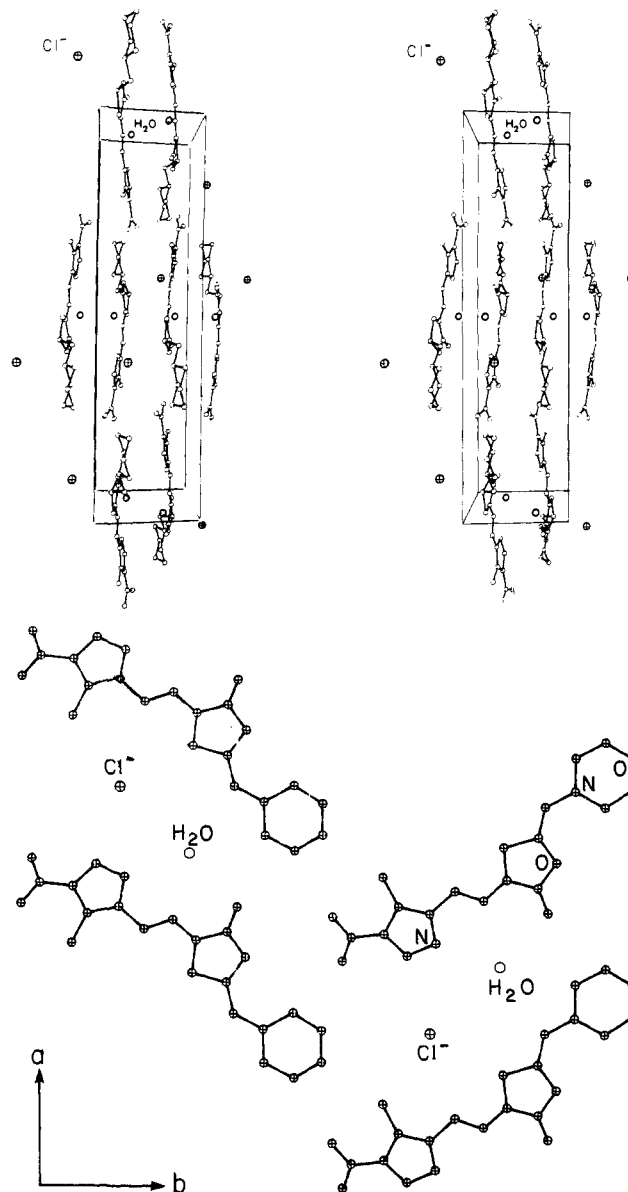


**Figure 7.** Crystal structure of moxnidazole hydrochloride monohydrate. (Top) A stereoview of the packing in the unit cell. (Bottom) Single molecular layer showing enclosure of  $\text{H}_2\text{O}$  in local intermolecular voids.

The clathration behavior of the furaltadone hydrochloride system appears to be mostly a mechanical phenomenon. Inspection of the data given in Table I suggests clearly that this host also forms an isomorphous clathrate-type complex with propionic acid (II). Furthermore, there are indications from powder diffraction spectra that butyric acid can be complexed by the same host structure. As indicated above (Table I), this lattice provides considerably flexible channels, expanding mainly in the  $b$  direction upon inclusion of increasingly larger species, in the order water < acetic acid < propionic acid. The above interesting observations call for further recrystallization experiments with guests of varying size (including long chain molecules) in order to define the limiting factors of this flexibility and to examine whether the host lattice may have any stereospecific function. It can be expected that larger chemically active guest constituents will form more stable clathrate structures with furaltadone hydrochloride. The apparent ability of the clathrate lattice to isolate monomeric species that in solution are present only in equilibrium with hydrogen-bonded dimers requires further investigation.

**Acknowledgment.** I am grateful to TEVA Pharmaceutical Industries, Ltd., for providing the materials and for financial support. I also thank Dr. Stephen Cherkez for stimulating dis-

cussions. This work was also supported in part by the Israel Commission for Basic Research. All calculations were carried out with the CDC 6600 computer of the Tel-Aviv University Computation Center.

Registry No. I, 83220-87-5; II, 83220-88-6; III, 83220-89-7; IV,

139-91-3; V, 83220-90-0; VI, 83220-91-1.

**Supplementary Material Available:** Tables of bond distances and angles (Tables VII, VIII, and IX), as well as tables of anisotropic thermal parameters (8 pages). Ordering information is given on any current masthead page.

## Gas-Phase Heteroaromatic Substitution. 2.<sup>1</sup> Electrophilic Methylation of Pyrrole and *N*-Methylpyrrole by $\text{CH}_3\text{XCH}_3^+$ ( $\text{X} = \text{F}$ or $\text{Cl}$ ) Ions

Giancarlo Angelini, Cinzia Sparapani, and Maurizio Speranza\*

Contribution from the Istituto di Chimica Nucleare del C.N.R., Area della Ricerca di Roma, C.P. 10, Rome, Italy. Received September 17, 1981

**Abstract:** The gas-phase methylation of pyrrole (**1**) and *N*-methylpyrrole (**2**) by  $\text{CH}_3\text{XCH}_3^+$  ( $\text{X} = \text{F}$  or  $\text{Cl}$ ) ions, from the  $\gamma$  radiolysis of  $\text{CH}_3\text{X}$ , has been investigated at pressures ranging from 50 to 760 torr, in the presence of a thermal radical scavenger ( $\text{O}_2$ ) and variable concentrations of an added base ( $\text{NMe}_3$ ). Both the reactivity of the selected pyrroles relative to benzene, used as the reference substrate in competition experiments, and the isomeric distribution of their methylated derivatives depend markedly on the total pressure of the system and the concentration of  $\text{NMe}_3$ . The apparent  $k_p/k_B$  ratios increase from 0.2 (**1**)-0.3 (**2**), in neat  $\text{CH}_3\text{F}$  at 50 torr, to over 0.4 (**1**)-1.0 (**2**), at 760 torr containing 10 torr of  $\text{NMe}_3$ . Concurrently, the isomeric distribution of the methylated products changes from  $\beta:\alpha:\text{N} = 80\%:13\%:7\%$  (from **1**) and  $\beta:\alpha = 65\%:35\%$  (from **2**) to  $\beta:\alpha:\text{N} = 50\%:15\%:35\%$  and  $\beta:\alpha = 70\%:30\%$ . These results are consistent with a methylation mechanism involving kinetically predominant  $\text{CH}_3\text{FCH}_3^+$  attack on the  $\beta$ -carbons of the pyrrolic substrate and subsequent isomerization of the resulting excited intermediates to the thermodynamically most stable 3-methylpyrrole protonated on the 2-position. The substrate and positional selectivity of the gas-phase methylation and the mechanism of isomerization that appears of intramolecular nature are discussed in the light of recent theoretical predictions on heteroaromatic reactivity and compared with the available data of related methylation reactions, occurring both in the gaseous and condensed phase.

Electrophilic substitution of five-membered heteroaromatic rings is a challenging area within which the modern concepts of theoretical chemistry and chemical reactivity find not only their widest application but also their inherent limits. Despite intense kinetic and mechanistic investigations, very few quantitative data are available that allow for a direct evaluation of the reactivity scale of simple heteroaromatics. The data accumulated show that, in solution, heteroaromatic reactivity may span over many orders of magnitude with the sequential hierarchy *N*-methylpyrrole > pyrrole >> furan > thiophene > benzene.<sup>2</sup> However, no reasonable explanation for this behavior has been so far presented. Certainly, environmental factors play a decisive role in determining such a large reactivity difference. The current literature of the field is studded with evidence for profound environmental effects on the magnitude of simple physical properties of fundamental heteroaromatics that are related to their electron density distribution (e.g., the overall dipole moment). These physical alterations are reflected in dramatic effects of the reaction medium upon the reactivity features of the heteroaromatic compounds. As a consequence, most of the heteroaromatic reactivity scales from solution studies are devoid of any quantitative significance since they originate from kinetic measurements carried out under diverse environmental conditions.<sup>2,3</sup> Environmental factors often de-

termine the directive properties of a given heteroaromatic ring toward electrophilic attack as well, although  $\alpha$  substitution appears to be a general rule in solution.

From the above considerations, a detailed investigation on the reactivity features of simple five-membered heteroaromatics toward electrophilic substitution would be of special interest if carried out in the dilute gas state, where complications related to the solvent, catalyst, counterion, etc. are completely eliminated. Under such conditions, in fact, direct evaluation of the intrinsic reactivity scale of simple heteroaromatics would be at hand. The absence of environmental effects also means that the results of the gas-phase investigation can be used with some confidence for testing the validity of the theoretical predictions on the reactivity and selectivity features of heteroaromatic compounds.<sup>4-7</sup>

(3) (a) Acheson, R. M. "An Introduction to the Chemistry of Heterocyclic Compounds", 2nd Ed; Wiley: New York, 1967. (b) Robert, J. D.; Caserio, M. C. "Basic Principles of Organic Chemistry"; W. A. Benjamin: New York, 1964. (c) Paquette, L. A. "Principles of Modern Heterocyclic Chemistry"; W. A. Benjamin: New York, 1968.

(4) (a) Abronin, I. A.; Belenkil, L. I.; Gol'dfarb, Ya. L. "New Trends in Heterocyclic Chemistry"; Elsevier: North-Holland, 1979. (b) Ridd, J. *Phys. Methods Heterocycl. Chem.* 1971, 55-120. (c) Jones, R. A.; Bean, G. P. "The Chemistry of Pyrroles"; Academic Press: New York, 1977.

(5) (a) Eplotts, N. D.; Cherry, W. R.; Bernardi, F.; Hehre, W. J. *J. Am. Chem. Soc.* 1976, 98, 4361-4364. (b) Gleghorn, J. T. *J. Chem. Soc., Perkin Trans. 2* 1972, 479-482.

(6) (a) Catalan, J.; Yanez, M. *J. Chem. Soc., Perkin Trans. 2* 1979, 1627-1631. (b) Palmer, M. H.; Gaskell, A. J. *Theor. Chim. Acta* 1971, 23, 52-58. (c) Kramling, R. W.; Wagner, E. L. *Ibid.* 1969, 15, 43-56.

(7) (a) Politzer, P.; Weinstein, H. *Tetrahedron* 1975, 31, 915-923. (b) Chou, D.; Weinstein, H. *Ibid.* 1978, 34, 275-286. (c) Politzer, P.; Donnelly, R. A.; Daiker, K. C. *J. Chem. Soc., Chem. Commun.* 1973, 617-618. (d) Berthel, G.; Bonaccorsi, R.; Scrocco, E.; Tomasi, J. *Theor. Chim. Acta* 1972, 26, 101-105.

(1) Presented in part at the 8th International Congress of Heterocyclic Chemistry, Graz, Austria, Aug 1981. Part I: Speranza, M. *J. Chem. Soc., Chem. Commun.* 1981, 1177-1178.

(2) For comprehensive reviews, see: (a) Marino G. *Adv. Heterocycl. Chem.* 1971, 13, 235-314. (b) Katritzky, A. R.; Lagowsky, J. M. "The Principles of Heterocyclic Chemistry"; Academic Press: New York, 1968. (c) Albert, A. "Heterocyclic Chemistry", 2nd ed; Oxford University Press: New York, 1968. (d) Jones, R. A. *Adv. Heterocycl. Chem.* 1970, 11, 383.